Oxidation and self-healing behaviour of spark plasma sintered Ta_2AlC

Farle, Ann Sophie M; Stikkelman, Julia; van der Zwaag, Sybrand; Sloof, Willem G.

DOI
10.1016/j.jeurceramsoc.2017.01.004

Publication date
2017

Document Version
Final published version

Published in
Journal of the European Ceramic Society

Journal of the European Ceramic Society 37 (2017) 1969–1974

Contents lists available at www.sciencedirect.com

Journal of the European Ceramic Society

journal homepage: www.elsevier.com/locate/jeurceramsoc

Oxidation and self-healing behaviour of spark plasma sintered Ta_2AlC

Ann-Sophie M. Farle[a,*], Julia Stikkelman[a], Sybrand van der Zwaag[b], Willem G. Sloof[a]

[a] Department of Materials Science and Engineering, Delft University of Technology, Mekelweg 2, 2628 CD, Delft, The Netherlands
[b] Faculty of Aerospace Engineering, Delft University of Technology, Kluyverweg 1, 2629 HS, Delft, The Netherlands

ARTICLE INFO

Article history:
Received 4 November 2016
Received in revised form
23 December 2016
Accepted 3 January 2017
Available online 10 January 2017

Keywords:
Ta_2AlC MAX phase
Spark plasma sintering
Self-healing
Oxidation

ABSTRACT

Self-healing and oxidation of spark plasma sintered Ta_2AlC was investigated using a newly developed wedge loaded compact specimen to determine strength recovery in a single specimen. Previous work had predicted dominant Al oxidation leading to dense and strong reaction products to result in favourable healing properties. However, crack-gap filling and strength recovery of Ta_2AlC were not achieved by oxidation at 600 °C. Oxidation below 900 °C in synthetic and atmospheric air resulted in porous Ta-oxides, with no Al_2O_3 formation. DTA up to 1200 °C revealed a two-step reaction process with the final products Ta_2O_5 and $TaAlO_4$. The study shows that the kinetics may overrule the self-healing MAX-phase design criteria based on thermodynamics.

1. Introduction

$M_{n+1}AX_n$ phases, with n equalling 1, 2, 3, or higher, are composed of transition metals (M), elements from groups 12–16 (A) and Carbon or Nitrogen (X) and belong to the family of metallo-ceramics. The atomic layered structure results in a unique combination of mechanical, thermal and electric properties. Recently it has been shown that some MAX phases demonstrate high temperature self-healing behaviour [1,2] when exposed to oxygen containing atmospheres. The healing behaviour of the self-healing MAX phases, such as Ti_2AlC, Ti_3AlC_2 and Cr_2AlC, is the result of a well-adhering Al_2O_3 layer forming at the two opposing crack faces [3–5]. In-situ time-resolved high-resolution synchrotron 3D X-ray tomography [6] revealed the actual crack filling process with sub-micron resolution. The study demonstrated that the crack closure is not restricted to the crack mouth but proceeds along the crack faces into the depth of the sample. Because of the almost complete filling of the crack with well adhering and dense high strength Al_2O_3 the healing process can lead to a full recovery of 4-point bending strength [3].

Furthermore, the healing process does not rely on the presence of external healing particles, but is a response of the material itself. Healing of a specific crack can take place several times and significant strength recovery even after 6 successive fracturing and healing steps has been demonstrated for Ti_2AlC [7]. Such a multiple healing ability is crucial for the successful introduction of the material in real-life engineering components operating at high temperatures and high loads, such as turbine engines. This potential has been demonstrated convincingly even under such harsh conditions [8].

Farle *et al.* [9] analysed the relevant parameters and phenomena in the known self-healing MAX phases and defined the following parameters as being crucial for obtaining high temperature oxidative self-healing behaviour: formation of a stable (non-oxygen transparent) oxide upon selective oxidation of the A-element, a relatively high diffusivity of the A-element to ensure fast oxidation, a sufficient volume expansion to fill a crack gap and a good adhesion of the oxide product to the matrix, as well as comparable coefficients of thermal expansion (CTE) and Young's Moduli of the healing product to those of the parent MAX phase. In these design rules, kinetic aspects were not taken into account.

Applying these criteria to the 79 known MAX phases returned the known self-healing grades (Ti_2AlC, Ti_3AlC_2 and Cr_2AlC) but also identified Ta_2AlC as a potential self-healing MAX phase. The analysis showed that Al_2O_3 over Ta_2O_5 should form, in which case there is a substantial volume increase, good adhesion and matching Young's Modulus and coefficient of thermal expansion. Earlier oxidation studies of Ta_2AlC have shown the formation of protective oxide layers is restricted to a narrow temperature window up to 600 °C [11].

The current study aimed to check and quantify the healing ability of spark plasma sintered Ta_2AlC and the underlying oxidation mechanisms. A newly-developed wedge loaded compact specimen configuration was used to measure strength recovery after 16 h of

* Corresponding author.
E-mail address: a.m.farle@tudelft.nl (A.-S.M. Farle).

http://dx.doi.org/10.1016/j.jeurceramsoc.2017.01.004
0955-2219/

oxidation in air. By inducing a path-controlled crack in a brittle material, self-healing strength recovery could be measured in a single sample, effectively reducing material consumption. To explain the absence of self-healing, oxide morphology, reaction energies and oxidation behaviour were assessed by thermal gravimetric and differential analysis over a wider temperature regime.

2. Experimental

Samples were prepared by spark plasma sintering (SPS) of Ta (>99.9%, <100 μm, ChemPur, Germany), Al (99.8%, 45 μm, TLS Technik GmbH &Co, Germany) and graphite (>99.5%, 6 μm, Graphit Kropfmuhl AG, Germany) powders in the ratio of 2:1.2:1. The starting powders were mixed for 12 h in a Turbula T2C Mixer (Willy A. Bachofen, Switzerland) using 5 mm ZrO_2 balls in a ratio of 10:1. Sintering was carried out in a spark plasma sintering furnace (Type HP D 25, FCT-Systeme GmbH, Germany) using graphite moulds of 20 and 40 mm diameter to create samples of approx. 5 mm thickness. The heating rate to the peak temperature of 1400 °C was 50 °C/min. The subsequent cooling rate was 100 °C/min. A pressure of 50 MPa was applied after heating to 700 °C and during sintering. To counteract the effects of Al loss while sintering at high temperatures, Al was taken to be over-stoichiometric in the initial mixture. Furthermore, pressureless heating up to 700 °C was applied to allow formation of solid intermetallics such as Ti_5Al_3 and prevent squeezing out of liquid aluminium formed around 660 °C.

In addition to the SPS experiments attempts were made to synthesise Ta_2AlC via pressureless sintering, however these did not yield pure MAX-phase powders, even when using the same composition and temperatures successfully employed during spark plasma sintering.

Self-healing of ceramics and MAX phases is commonly tested by four- or three-point bending, resulting by definition in a relatively high material consumption [11], as monitoring of strength recovery in an individual fractured sample is impossible. To track the oxidation induced strength recovery of Ta_2AlC in the same sample, a modified chevron notched compact specimen was used.

Self-healing efficiency was determined using a newly developed dedicated chevron notched, wedge loaded specimen (WLS) geometry, whereby a 10° quenched and tempered steel wedge was used for load application to create a crack along a designated path in a 24 × 25 mm sample with a rounded bottom and a chevron notch, see Fig. 1. Tests were performed using a 100 kn electro-mechanical load frame (Instron, type 5500R) which was fitted with a 10 kn load cell. Wedge displacement was stopped upon a specified (50%) load drop to arrest the crack before full fracture of the sample. Tests were carried out under closed loop displacement control, with a fixed crosshead displacement rate of 0.1 mm/s. The crack length was determined ex-situ by optical microscopy using a digital microscope (Keyence VHX-100, Osaka, Japan) and scanning electron microscopy.

Cracks were healed ex-situ at 600 °C for 16 h in atmospheric air using an alumina tube furnace (LTF 16/75/610, Lenton, UK) before the wedge loading test was repeated under the conditions of the first loading. The healing temperature was based on observations by Gupta *et al.* [10].

For microstructural analysis all samples were ground and polished using SiC abrasive paper up to 2500 grit and diamond paste up to 0.25 μm. Quantitative compositional analysis of the synthesised MAX phase as well as the oxidation products was carried out by electron probe X-ray micro analysis (EPMA) using a JXA-8900R superprobe (JEOL Ltd., Japan) equipped with wave dispersive spectroscopy (WDS). Measurements were performed on carbon coated samples using an electron beam with 10 keV energy and a beam current of 50 nA. Decontamination of measurement spots

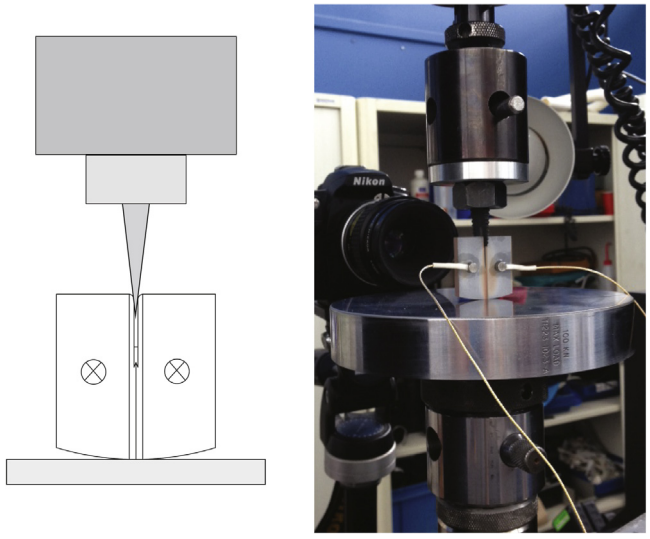

Fig. 1. Test setup of wedge loaded chevron notched specimen with microphone positions indicated (a) schematic and (b) actual test setup.

was achieved using an air-jet. The composition at each analysis location of the sample was determined using the X-ray intensities of the constituent elements after background correction relative to the corresponding intensities of reference materials. The thus obtained intensity ratios were processed with a matrix correction program CITZAF [12].

Furthermore, oxide morphology, scale thickness and homogeneity were investigated by scanning electron microscopy using a JSM 6500F microscope (JEOL Ltd., Tokyo, Japan). This microscope is equipped with an energy dispersive x-ray spectrometer (EDS) (ThermoFisher UltraDry 30 mm^2 detector) for X-ray microanalysis (XMA). Data acquisition and analysis was carried out with Noran System Seven software package (Thermo Electron Scientific Instruments LLC., USA).

Isothermal oxidation kinetics were investigated by thermal gravimetric analysis (TGA) using a high performance symmetrical TGA system (TAG 16/18, Setaram Instrumentation, Caluire, France) to eliminate buoyancy effects. Bulk samples (3 × 4.5 × 12.5 mm), suspended from sapphire rods, were oxidized for 10 h at 600, 700 and 800 °C in a flow of dry artificial air composed of 40 sccm N_2 (purity > 5N) and 10 sccm O_2 (purity > 5N). Prior to oxidation all samples were manually ground with SiC paper of increasing fineness up to 2500 grit and cleaned in acetone. Heating and cooling of all samples was conducted in Ar (purity > 5N, 50 sccm) atmosphere.

Necessary machining for TGA and the modified chevron notched compact specimen was carried out by electronic discharge machining (EDM) with wire diameters of 0.25 and 0.1 mm.

Differential thermal analysis (TGA/DTA) was performed using a SETSYS Evolution 1750 (Setaram, Caluire, France) coupled with mass spectrometry (OmniStar™, GSD 301 O, Pfeiffer Vacuum, Asslar, Germany) to detect CO_2 evolution. Powdered samples of Ta_2AlC were heated to 1200 °C with different heating rates (1, 2, 5, 10, 15 °C/min) in a flow of pure dry synthetic air, i.e. 40 sccm N_2 (purity > 5N) and 10 sccm of O_2 (purity > 5N). The recorded data was corrected for buoyancy effects by subtraction of a blank measurement performed under the same conditions. Weight gain was normalized to a range of 0–1, corresponding to the maximum weight gain of 6.7 mg. Powders were obtained by pulverizing dense bulk SPS samples using a variable speed rotary tool (Dremel 395, Dremel, USA) with a clean diamond tip. The resulting powder was characterized by SEM and laser diffraction particle size analysis (Mastersizer X, Malvern Instruments, UK). The average powder size was 210 μm.

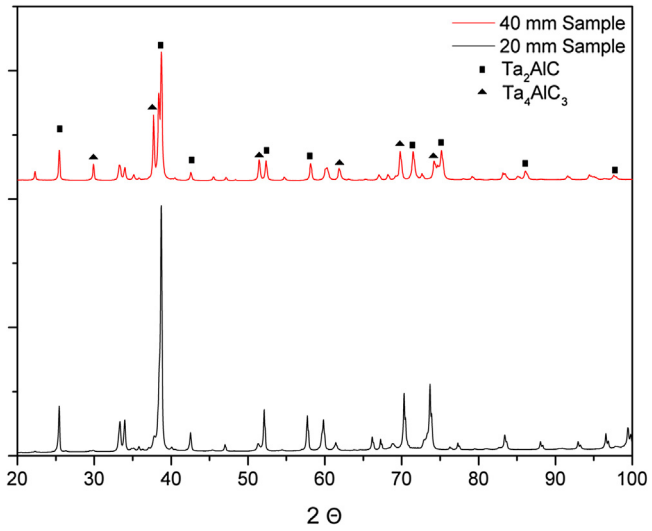

Fig. 2. XRD patterns of spark plasma sintered Ta_2AlC with varying Ta_4AlC_3 content for two samples sizes.

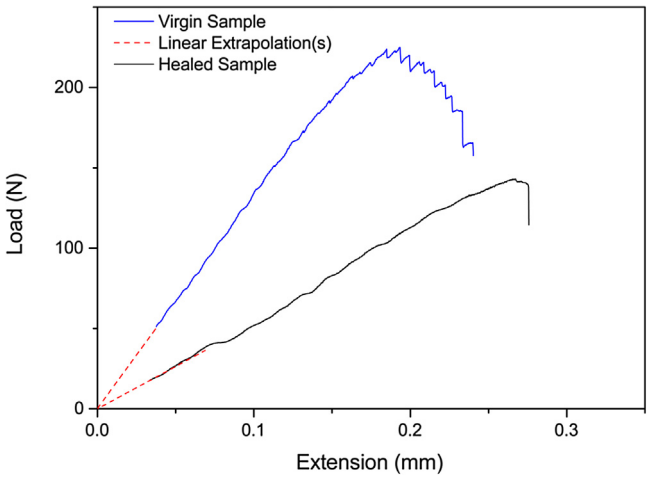

Fig. 3. Load versus displacement curves of wedge loaded chevron notched Ta2AlC specimen before and after isothermal oxidation at 600 °C for 16 h in air. Samples were pre-loaded to approx. 20 and 55 N, thus both curves were extrapolated for better comparison.

The DTA results were analysed using the so-called Kissinger-Sunose-Akahira equation [13]:

$$\ln\left(\frac{\beta}{T_P^2}\right) + \frac{E_A}{RT_p} = \text{constant} \quad (1)$$

where E_A is the activation energy, R is the gas constant, T_p the peak temperature and β the heating rate. The slope of the straight line fitted to the data points for $ln(\beta/T_p^2)$ versus $1/T_p$ yields the activation energy of the reaction.

3. Results and discussion

For the optimal SPS conditions, listed above, homogeneous, dense material, free of internal defects was obtained. The same synthesis procedure employed for all samples resulted in compositional variations between the samples of different sizes. Fig. 2 shows two XRD patterns, of a 20 mm and a 40 mm sample. Both contain Ta_4AlC_3, another MAX-phase configuration as a second phase, whereby 20 mm samples contain approx. 10% and the larger samples up to 50%. The 40 mm samples were used for crack healing tests and the 20 mm samples for TGA and DTA.

The difference in mould size did not affect the microstructure of the samples. Elongated grains of 20–40 μm in length, with completely random orientation, were identified in all samples.

Load-displacement curves of the wedge loaded compact specimen, recorded before and after oxidation showed a large difference in the slope during initial loading, see Fig. 3. This is attributed to a change in the friction coefficient between the wedge and sample upon oxidation. Furthermore, softening of the material seemed to occur.

Wedge loading of the chevron notched compact specimen led to stable crack growth and a peak load of 225 N for the virgin material. After the load dropped to 157 N the wedge was retracted and the samples were examined, revealing a crack with the length of 8.3 mm and a width of up to 5 μm, approx. 55% of the available sample length. The crack morphology was as that commonly observed in MAX phase materials [3].

Loading of the sample healed at 600 °C for 16 h was resumed. However, the maximum load did not exceed 143 N, which is below the residual load-bearing capacity of the virgin material, see Fig. 3. Hence, no strength recovery was achieved by oxidation at 600 °C for 16 h.

SEM images of an oxidized specimen before re-cracking show an oxidized zone of approx. 60 μm thickness on both crack surfaces after 16 h at 600 °C. The crack gap is flanked by porous Ta-oxide on top of the original matrix material. As can be seen in Fig. 4, convergence of the crack walls could not be detected. Fig. 4b shows the oxidation proceeding along the grain boundaries, enveloping areas of virginal material. Furthermore, the oxidation progresses exclusively inward from the fracture surfaces.

The absence of Al_2O_3 and thus strength recovery, supports the necessity for further oxidation studies. Supplementary thermogravimetric analysis of bulk Ta_2AlC at 600, 700 and 800 °C for 10 h supports the observations of the wedge intrusion test. 10 h of oxidation at 600 °C did not result in a porous or pronounced oxide layer, however oxidation at 700 and 800 °C similar morphology to the sample treated at 600 °C for 16 h. Fig. 5 shows the weight

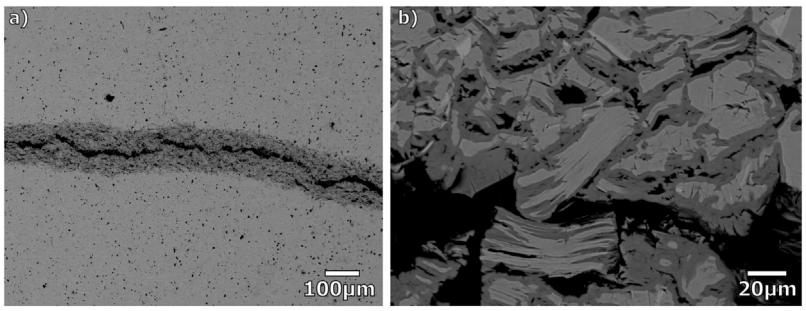

Fig. 4. Backscattered electron image of Ta_2AlC oxide after 16 h of oxidation at 600 °C.

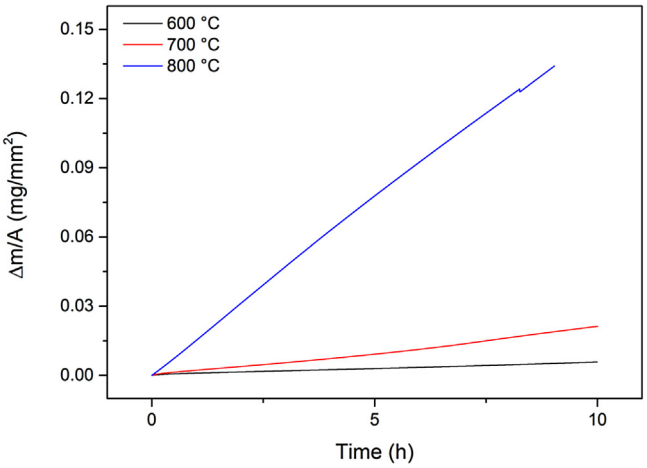

Fig. 5. Weight gain of Ta_2AlC at 600, 700 and 900 °C for 10 h.

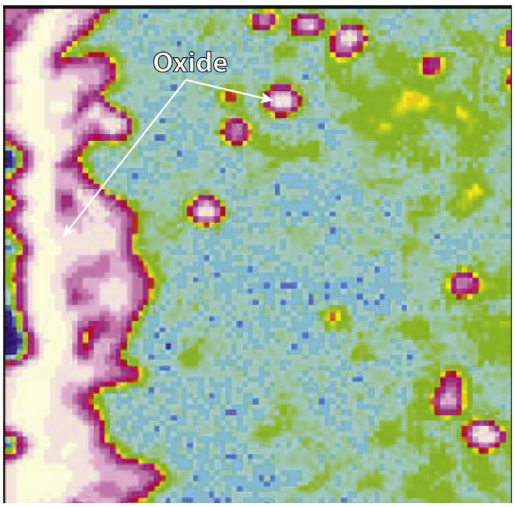

Fig. 6. Qualitative EPMA map of oxygen in Ta_2AlC oxidized at 600 °C for 10 h.

gain of bulk Ta_2AlC for oxidation at different temperatures for 10 h. Isothermal oxidation of bulk Ta_2AlC with Ta_4AlC_3 impurities (cf. Fig. 2) revealed nearly linear oxidation kinetics at all tested temperatures, i.e. 600, 700 and 800 °C.

XRD could not detect any oxide formed at 600 °C after 10 h. SEM and SEM-XMA however show a 2–5 μm thick oxygen enriched Ta-Al layer with molar ratios of Ta:Al:O = 2.5:1:6. Qualitative EPMA measurements display an up to 6 μm thick oxygen enriched area; see Fig. 6.

SEM and EPMA measurements show areas of original MAX phase composition within the oxidized region after oxidation at 700 °C, see Fig. 7b. Comparable morphology can be seen after isothermal oxidation at 800 °C, where the porous oxide layer has increased up to 250 μm in thickness, but no longer contains original MAX phase material (Fig. 7c). The oxide developed after 10 h of oxidation at 800 °C is composed of TaO, $TaO_{1,67}$ and Ta_2O_5, as determined by XRD analysis. In contrast to the predictions based on postulated criteria [9] no Al based oxides were identified.

Oxidation of pure Ta_2AlC and Ta_2AlC/Ta_4AlC_3 samples, revealed no significant difference in oxide composition or morphology. Furthermore, the oxide scales documented by Gupta *et al.* [10] are seemingly identical to those shown here. This indicates that minor compositional changes or synthesis routes do not affect the overall oxidation behaviour of Ta-Al-C MAX-phases.

Sufficient volume expansion upon oxidation of Al was a design criterion for effective self-healing of Ta_2AlC [9]. However, the formation of Ta-oxides leads to highly porous and cracked oxides due to the large volume expansion upon oxidation of Ta_2AlC to Ta_2O_5, and possibly $TaAlO_4$. The relative volume expansion upon oxidation (RVE) [9] was determined for two cases: i.e. the conversion of MAX phase into Ta_2O_5 only, and conversion of MAX phase into Ta_2O_5 and the maximum possible amount of $TaAlO_4$, based on stoichiometry (see Eqs. (2) and (3)). All values calculated lie above 1.5, viz.: 1.55 and 2.0 for the full or combined oxidation of Ta_2AlC, and 1.77 and 2.02 for Ta_4AlC_3.

$$RVE = \frac{V_{Ta_2O_5}}{V_{Ta_xAlC_y}} \tag{2}$$

$$RVE = \frac{xV_{Ta_2O_5} + 2V_{TaAlO_4}}{2V_{Ta_xAlC_y}} \tag{3}$$

The high RVE corresponds well with the observed microstructure of the oxide scales on TGA samples after isothermal oxidation at 700 and 800 °C. Furthermore, cracks in the oxides could be a result of the thermal mismatch between Ta-oxides and the MAX phase, i.e. the CTE of Ta_2O_5 is reported to be between 2.9 and $4.0 \times 10^{-6}\ K^{-1}$ while the measured dilatometric thermal expansion coefficient (TEC) of Ta_2AlC is $6.0 \times 10^{-6}\ K^{-1}$ [10,14]. With the exception of no solid Al_2O_3 layer, all criteria for self-healing are met. The absence of the healing effect due to porous Ta-oxides must be due to kinetics.

According to the DTA measurements shown in Fig. 8 the oxidation of Ta_2AlC proceeds in a two-step process. For a heating rate of 5 °C/min the first reaction peaks at approx. 760 °C. X-ray diffraction of powders retrieved at 800 °C show that the MAX phase has partially oxidized into $TaO_{1.1}$ and $Ta_{1.86}Al_{0.14}O_{4.86}$. The unreacted Carbon remains in Ta_4C_3 and Ta_2AlC.

The second exothermal peak is attributed to the oxidation of Carbon from Ta_4C_3 and/or Ta_2AlC to CO_2. Powders retrieved after heating up to 1200 °C show full conversion to Ta_2O_5 and $TaAlO_4$. The conversion from the initial oxides $TaO_{1.1}$, $Ta_{1.86}Al_{0.14}O_{4.86}$ and the remaining Ta_4C_3 and Ta_2AlC to Ta_2O_5 and $TaAlO_4$ takes place at approx. 850 °C under loss of C to form CO_2, see Fig. 8. Mass spectrometry revealed the reaction of Carbon to CO_2 during oxidation, confirming a long-standing assumption for MAX-phase oxidation [15].

The formation of Al containing oxides such as $Ta_{1.86}Al_{0.14}O_{4.86}$ and $TaAlO_4$ was not observed for bulk oxidation (TGA) at 600, 700 or 800 °C.

The activation energy (E_a) of the initial decomposition reaction of Ta_2AlC into $TaO_{1.1}$ and $Ta_{1.86}Al_{0.14}O_{4.86}$ was calculated using the Kissinger-Sunose-Akahira equation [13], relating the peak temperatures of reactions measured for different heating rates to their activation energy, see Fig. 9. This resulted in a value for the activation energy of 146 ± 10 kJ/mol. Though data should be treated with care, because activation energies calculated by method of Kissinger-analysis based on DTA data are only valid for simple decomposition reactions, regardless the order of the reaction [13].

The activation energy can now be compared with those of other related materials. The activation energy of 146 ± 10 kJ/mol, required for oxidation of Ta_2AlC lies below that of Ti_2AlC, Ti_3SiC_2, Ta and TaC, viz.: 363 [8], 325 [5], 183 ± 8 [16] and 379 ± 16 [17] kJ/mol, respectively. It is most comparable to that of Ta_2C with 129 ± 7 kJ/mol [17].

The similarity in activation energy and oxide morphology [17] of Ta_2AlC and Ta_2C oxidation emphasises that Al does not substantially contribute to the oxidation reaction. Tantalum oxide formation is dominant, possibly also due to its abundance and higher activity in Ta_2AlC or Ta_4AlC_3 than Al.

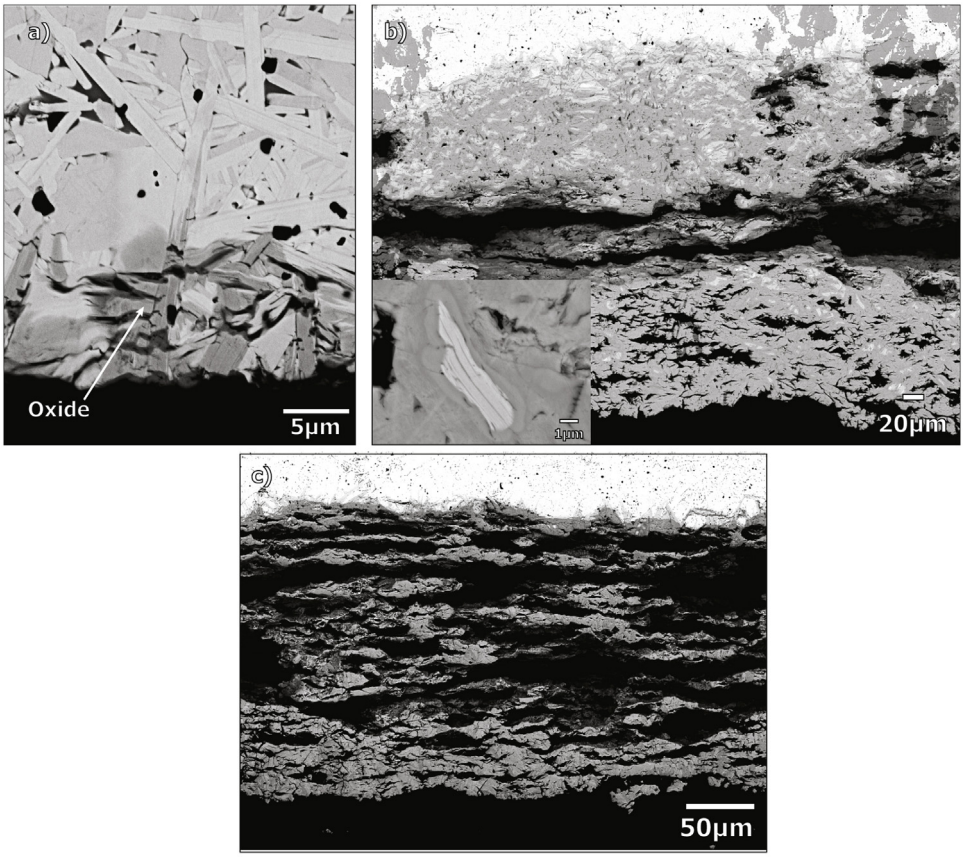

Fig. 7. SEM images of oxide scales after 10 h of isothermal oxidation of Ta_2AlC in artificial air at a) 600, b) 700 and c) 800 °C.

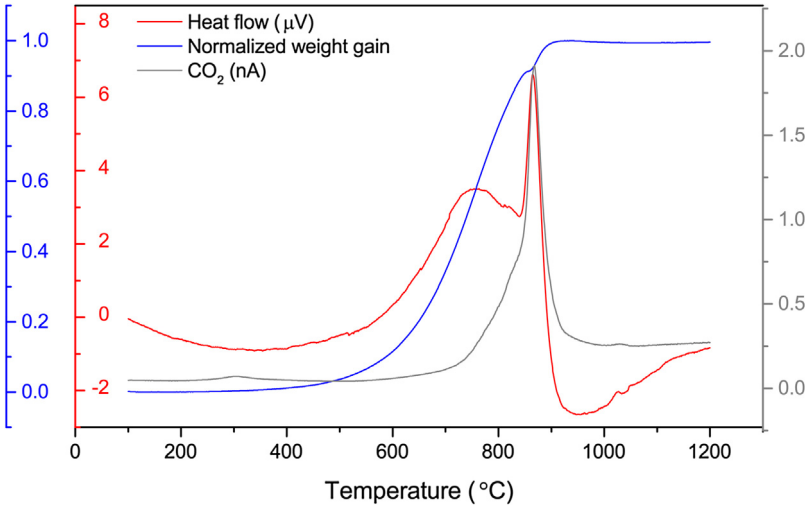

Fig. 8. Heat flow, mass gain (TG) and CO_2 signal of Ta_2AlC powder heated up to 1200 °C with 5 °C/min.

Finally, thermodynamic data can be considered insufficient for oxide prediction without supportive kinetic data. Previous work had assumed the internal diffusion of the A-element towards the oxidation front or crack gap would be a critical factor for competitive oxide growth, especially in self-healing compounds [9]. However, initial oxidation of all constituents should be considered and the consequential oxidation limited by O_2 diffusivity and M- and A-element mobility should be among the determining factors for final oxide prediction. The authors recommend an inclusion of diffusion data, viz.: A in M-oxides, and especially the O_2 transport.

4. Conclusions

Self-healing of Ta_2AlC by means of a wedge loaded specimen and thermal treatment at 600 °C did not result in strength recovery. Oxidation studies showed Ta-oxide formation with an activation energy of 146 ± 10 kJ/mol, resulting in highly porous oxide scales. The thermodynamically predicted Al_2O_3 formation was not observed at temperatures up 1200 °C. The study provides proof that kinetic data should be added to the list of design criteria for self-healing MAX phases.

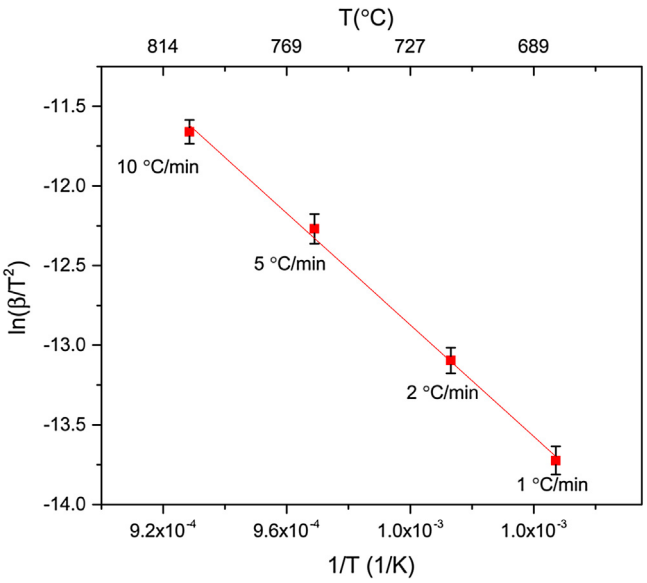

Fig. 9. Kissinger points and linear fit of 1st reaction from DTA data on Ta_2AlC heated with 1, 2, 5 and 10 °C/min.

Acknowledgements

This research was sponsored by the People Programme (MarieCurie ITN) of the European Union's seventh framework programme, FP7, grant number 290308 (SHeMat). The authors would like to thank Hans Brouwer for technical support with the SPS and TG-DTA experiments, Kees Kwakernaak for the EPMA measurements and Ruud Hendrix for XRD analysis.

References

[1] M.W. Barsoum, The $M_{(N+1)}AX_{(N)}$ phases: a new class of solids; thermodynamically stable nanolaminates, Prog. Solid State Chem. 28 (2000) 201–281.
[2] W. Sloof, A. Farle, L. Shen, Intrinsic autonomous crack healing in MAX phase ceramics, in: S.v.d. Zwaag, E. Brinkman (Eds.), Self-healing Materials – Pioneering Research in the Netherlands, IOP Press, 2015, 2017, pp. 115–123.
[3] G.M. Song, Y.T. Pei, W.G. Sloof, S.B. Li, J.T.M. De Hosson, S. van der Zwaag, Oxidation-induced crack healing in Ti_3AlC_2 ceramics, Scr. Mater. 58 (2008) 13–16.
[4] R. Pei, S. McDonald, L. Shen, S. van der Zwaag, W. Sloof, P. Withers, P. Mummery, Crack healing behaviour of Cr_2AlC MAX phase studied by X-ray tomography, J. Eur. Ceram. Soc. (2016) 441–450.
[5] S. Li, L. Xiao, G. Song, X. Wu, W.G. Sloof, S. van der Zwaag, Oxidation and crack healing behavior of a fine-grained Cr_2AlC ceramic, J. Am. Ceram. Soc. 96 (2013) 892–899.
[6] W.G. Sloof, R. Pei, S.A. McDonald, J.L. Fife, L. Shen, L. Boatemaa, A.-S. Farle, K. Yan, X. Zhang, S. van der Zwaag, P.D. Lee, P.J. Withers, Repeated crack healing in MAX-phase ceramics revealed by 4D in situ synchrotron X-ray tomographic microscopy, Sci. Rep. 6 (2016) 23040.
[7] S. Li, G. Song, K. Kwakernaak, S. van der Zwaag, W.G. Sloof, Multiple crack healing of a Ti_2AlC ceramic, J. Eur. Ceram. Soc. 32 (2012) 1813–1820.
[8] A.-S. Farle, L. Boatemaa, L. Shen, S. Gövert, J.B.W. Kok, M. Bosch, S. Yoshioka, S. van der Zwaag, W.G. Sloof, Demonstrating the self-healing behaviour of some selected ceramics under combustion chamber conditions, Smart Mater. Struct. 25 (2016) 084019.
[9] A.-S. Farle, C. Kwakernaak, S. van der Zwaag, W.G. Sloof, A conceptual study into the potential of $M_{n+1}AX_n$-phase ceramics for self-healing of crack damage, J. Eur. Ceram. Soc. 35 (2015) 37–45.
[10] S. Gupta, D. Filimonov, M.W. Barsoum, Isothermal oxidation of Ta_2AlC in air, J. Am. Ceram. Soc. 89 (2006) 2974–2976.
[11] ASTM C1421-16, Standard Test Methods for Determination of Fracture Toughness of Advanced Ceramics at Ambient Temperature, Standard, ASTM International, West Conshohocken, PA, USA, 2016.
[12] J.T. Armstrong, Quantitative Elemental Analysis of Individual Microparticles with Electron Beam Instruments Electron Probe Quantitation, Springer, 1991, pp. 261–315.
[13] H.E. Kissinger, Variation of peak temperature with heating rate in differential thermal analysis, J. Res. Nat. Bur. Stand. 57 (1956) 217–221.
[14] Y. Touloukian, R. Kirby, R. Taylor, T. Lee, Thermal Expansion-nonmetallic Solids, The TRPC Data Series, Vol. 13, Plenum, New York, 1977.
[15] M.W. Barsoum, MAX Phases: Properties of Machinable Ternary Carbides and Nitrides, Wiley-VCH, 2013.
[16] A. Beck, M. Heine, E. Caule, M. Pryor, The kinetics of the oxidation of Al in oxygen at high temperature, Corros. Sci. Elsevier 7 (1) (1967) 1–10.
[17] M. Desmaison-Brut, N. Alexandre, J. Desmaison, Comparison of the oxidation behaviour of two dense hot isostatically pressed tantalum carbide (TaC and Ta_2C) materials, J. Eur. Ceram. Soc. 17 (1997) 1325–1334.